




DYNAMIC MODEL FOR MEASLES INFECTION WITH SEIRV+D MODEL

Maja Kukuseva Paneva¹  [0009-0001-2556-3796], Natasha Stojkovic²  [0000-0003-2770-0771] and Vladimir Milićević^{3*}  [0000-0002-5587-2717]

¹ Faculty of Electrical Engineering, Goce Delcev University, Stip, North Macedonia
e-mail: maja.kukuseva@ugd.edu.mk

² Faculty of Computer Science, Goce Delcev University, Stip, North Macedonia
e-mail: natasa.stojkovic@ugd.edu.mk

³ Faculty of Mechanical and Civil Engineering, Kraljevo, University of Kragujevac
e-mail: milicevic.v@mfkv.kg.ac.rs

*corresponding author

Abstract

This paper explores the dynamics and stability of measles infection within a specified population, utilizing the SEIRV+D model. The study commences by establishing the equilibrium points and determining the reproduction number. The stability of this equilibria is contingent on the calculated reproduction number. The research draws upon real data obtained by Public Health Institute of North Macedonia to conduct a case study. Various simulations are executed, examining a range of transmission and vaccination rates.

Keywords: dynamic model, measles infection, SEIRV+D model, reproduction number, equilibrium point.

1. Introduction

Measles is among the highly contagious infection diseases with a long history of presence in humans. It is caused by a virus from Morbillivirus genus, part of the Paramyxoviridae family (Griffin, 2016). The virus is spread through respiratory droplets, typically released by coughing, sneezing or close contact with an infected person.

The first effective measles vaccine was developed by Dr John Enders and colleagues in the 1960s (Berche 2022), laying the formulation for the development MRP vaccine. The introduction of the vaccine has significantly reduced the incidence of measles and its associated complications. The MRP vaccine is typically administered in two doses to children, with the first dose given around 12-15 months of age and the second dose from 4 to 6 years of age. High vaccination coverage helps establish community immunity, protecting those who cannot be vaccinated due to certain medical conditions. Despite vaccination efforts, measles still exists in some parts of the world, and the outbreaks can occur due to various factors. In the last decade, measles epidemic occurred in North Macedonia in 2014, 2017, 2018 and 2019. According to Public Health Institute (2023) in the 2018/2019 epidemic, 1901 individual was infected across 24 cities.

The transmission of many infectious diseases, including measles, influenza, COVID-19 and tuberculosis have been described using dynamic mathematical models. These models utilize mathematical equations to describe the interactions among various factors, aiding researchers and public health officials in understanding how diseases spread and in developing strategies to control the outbreak. The mathematical models are based on classical SIR (Susceptible, Infected, Recovered) model represented in Lau (2022) and Zaman (2017). The SEIR (Susceptible, Exposed, Infected, Recovered) model is adapted for diseases characterized by longer incubation periods and longer-lasting immunity, as discussed by Aarsal (2020), Ottar (2002) and Stojkovicj (2024). Most recently, SEIRV (or SVEIR) models and SEIRVS models have been deployed as by Kukusheva Paneva (2024). The influence of vaccination on measles transmission and dynamics is explored by Hajji (2022) and Al- Darabsah (2021).

The model deployed in this paper is a modification of the model represented by Kukusheva Paneva (2024) with the difference that the recruitment rate Λ is used instead of birth rate λ . In the paper by Kukusheva Paneva (2024) only the model and the reproduction number are given, where the reproduction number is not derived. The case study in that paper is conducted for a period of 5 years, whereas in our paper the case study is performed for twelve months. Also, the stability of the system and disease-free equilibrium point for the deployed model are represented. The proposed SEIRV+D model offers several benefits in analyzing the transmission of measles. By including the vaccination rates and the immunity development rate, the model enables the quantification of the impact of immunization programs. This model can represent real-world scenarios, illustrating the effectiveness of vaccination and its influence on disease-related mortality. The model also includes demographic factors, such as birth and death rates. These rates enable simulations that consider population changes and how those changes may affect disease spread over time. Additionally, the model considers the transmission rate, which highlights the effect on disease spread based on the number of contacts an infected individual has with other individuals. Another advantage of the model is its flexibility - any parameter can be adjusted, making it suitable for testing various scenarios. The model uses real data (e.g. from Public Health Institute of North Macedonia), enhancing its relevance and applicability.

The model also has certain limitations. It assumes that every individual interacts with an equal number of other individuals. This oversimplifies the real dynamics, especially in areas with varying population densities. Also, social distancing among individuals, the introduction of quarantines, or other measures applied during epidemics, which can significantly alter the disease's dynamics, are not considered in this model. Additionally, the model does not consider the effect of the age group and the comorbidities' infected individuals have on measles-related mortality.

2. Methods and materials

The research involves the development and analysis of SEIRV model which divides the total populations into six compartments at any given time: susceptible, exposed, infected, recovered, vaccinated and deceased:

$$N(t) = S(t) + E(t) + I(t) + R(t) + V(t) + D(t) \quad (1)$$

where time t is in months.

The susceptible compartment is affected by the recruitment rate Λ and the rate of ineffective vaccination σ . To achieve community immunity, WHO (2019) recommends 95% of the total population to be vaccinated. Vaccination is deemed ineffective when a fully vaccinated individual fails to develop immunity and returns to susceptible compartment. The rate of unsuccessful

vaccination according to Bailey (2023) is around 5% among all vaccinated individuals. Once fully vaccinated, the susceptible individuals' transit to vaccinated compartment at a vaccination rate q . Antibodies for measles typically appear between 12 and 15 days after vaccination, but sometimes between 21 and 28 days (Moss, 2006). The vaccinated individuals who develop immunity move to recovered compartment with successful vaccination rate v . Individuals from susceptible compartment may interact with infected individual and upon contact progress to exposed compartment with transmission rate β . Proportion of exposed individuals progress to infected compartment by incubation rate $\alpha = \frac{1}{\tau_{latent}}$, where τ_{latent} is the latent (incubation) period of measles and approximately last 10 days but can vary from 7 to 21 days upon exposure (CDC, 2021). Infected individuals who receive treatment and recover progress to recovered compartment with recovery rate $\gamma = \frac{1}{\tau_{recovery}}$. The time $\tau_{recovery}$ is recovery time of measles usually between 2 and 3 weeks, after which the individual is immune (resistant) to the measles virus. Infected individuals who die because of measles progress to death compartment with measles-related death rate δ . The susceptible, exposed, infected, vaccinated and recovery compartments are decreased with constant natural mortality rate denoted by μ . The deployed model is shown in Figure 1.

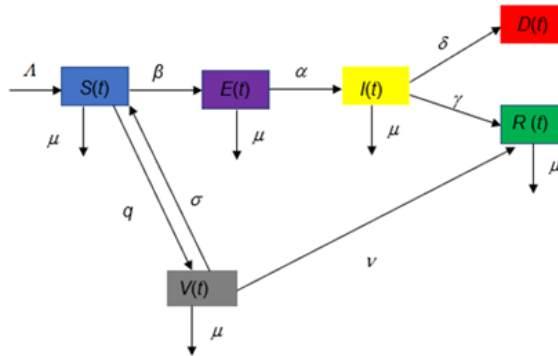


Fig. 1. Measles infection compartments model

The transmission dynamics of measles for this model can be represented with the system of stochastic differential equations as:

$$\begin{aligned}
\frac{dS(t)}{dt} &= \Lambda - \frac{\beta S(t)I(t)}{N} - qS(t) + \sigma V(t) - \mu S(t) \\
\frac{dE(t)}{dt} &= \frac{\beta S(t)I(t)}{N} - \alpha E(t) - \mu E(t) \\
\frac{dI(t)}{dt} &= \alpha E(t) - \gamma I(t) - \delta I(t) - \mu I(t) \\
\frac{dR(t)}{dt} &= \gamma I(t) + \nu V(t) - \mu R(t) \\
\frac{dV(t)}{dt} &= qS(t) - \sigma V(t) - \nu V(t) - \mu V(t) \\
\frac{dD(t)}{dt} &= \delta I(t)
\end{aligned} \tag{2}$$

Where the initial conditions are:

$$S(0) = S_0 \geq 0, E(0) = E_0 \geq 0, I(0) = I_0 \geq 0, R(0) = R_0 \geq 0, D(0) = D_0 \geq 0, V(0) = V_0 \geq 0. \tag{3}$$

Theorem 2.1. If the system given with Equation (2) is valid, then the bounded region for feasible solution with initial conditions (3) is:

$$\Omega = \left\{ x = (S, E, I, R, V, D) \in \mathbb{R}^6 : 0 \leq N \leq \frac{\Lambda}{\mu} \right\} \tag{4}$$

Proof 2.1. The total population for the deployed model is given by (1) and then:

$$\begin{aligned}
\frac{dN}{dt} &= \frac{dS}{dt} + \frac{dE}{dt} + \frac{dI}{dt} + \frac{dR}{dt} + \frac{dV}{dt} + \frac{dD}{dt} = \\
\Lambda - \mu(S + E + I + R + V) &= \Lambda - \mu(N - D)
\end{aligned} \tag{5}$$

Because of $D \ll N$, the equation (5) becomes:

$$\frac{dN}{dt} \approx \Lambda - \mu N$$

Then, it can be deduced that:

$$\frac{dN}{dt} \leq \Lambda - \mu N \tag{6}$$

By solving the following ordinary differential equation:

$$\begin{aligned}
\frac{dN}{dt} + \mu N &= \Lambda \\
N &= \frac{\Lambda}{\mu} + C_0 e^{-\mu t}
\end{aligned}$$

For initial condition $t = 0$:

$$N_0 = \frac{\Lambda}{\mu} + C_0 \Rightarrow C_0 = N_0 - \frac{\Lambda}{\mu}$$

$$\text{So, } N = \frac{\Lambda}{\mu} + \left(N_0 - \frac{\Lambda}{\mu} \right) e^{-\mu t} = N_0 e^{-\mu t} + \frac{\Lambda}{\mu} (1 - e^{-\mu t})$$

Because of (6):

$$N \leq N_0 e^{-\mu t} + \frac{\Lambda}{\mu} (1 - e^{-\mu t})$$

with taking $t \rightarrow \infty$ the following is obtained:

$$N \leq \frac{\Lambda}{\mu} \quad (7)$$

Thus, it is proved that (4) is bounded region.

Theorem 2.2. The equilibrium point for the model (2) is:

$$X^* = (S^*, E^*, I^*, R^*, V^*, D^*) = \left(\frac{\Lambda(\sigma + \nu + \mu)}{(q + \mu)(\sigma + \nu + \mu) - \sigma q}, 0, 0, \frac{\nu q \Lambda}{\mu[(q + \mu)(\sigma + \nu + \mu) - \sigma q]}, \frac{q \Lambda}{(q + \mu)(\sigma + \nu + \mu) - \sigma q}, 0 \right) \quad (7)$$

Proof 2.2. The equilibrium point is reached when all the equations form Equation (2) are set to zero.

$$\begin{aligned} \frac{dS}{dt} = \frac{dE}{dt} = \frac{dI}{dt} = \frac{dR}{dt} = \frac{dV}{dt} = \frac{dD}{dt} &= 0 \\ \Lambda - \frac{\beta SI}{N} - qS + \sigma V - \mu S &= 0 \\ \frac{\beta SI}{N} - \alpha E - \mu E &= 0 \\ \alpha E - \gamma I - \delta I - \mu I &= 0 \\ \gamma I + \nu V - \mu R &= 0 \\ qS - \sigma V - \nu V - \mu V &= 0 \\ \delta I &= 0 \end{aligned} \quad (8)$$

If the system is solved, from equation (8) for the pointes S^*, E^*, I^*, R^*, V^* and D^* follows:

$$\begin{aligned} S^* &= \frac{\Lambda(\sigma + \nu + \mu)}{(q + \mu)(\sigma + \nu + \mu) - \sigma q} \\ E^* &= 0 \\ I^* &= 0 \\ R^* &= \frac{\nu q \Lambda}{\mu[(q + \mu)(\sigma + \nu + \mu) - \sigma q]} \end{aligned}$$

$$V^* = \frac{q\Lambda}{(q + \mu)(\sigma + \nu + \mu) - \sigma q}$$

and

$$D^* = N^* - (S^* + E^* + I^* + R^* + V^*) = \frac{\Lambda}{\mu} - (S^* + E^* + I^* + R^* + V^*) = 0$$

From above equations, the total population is $N^* = \frac{\Lambda}{\mu}$ applying the equilibrium point. For disease-free equilibrium (DFE) point (7) is obtained.

The basic reproduction number \mathfrak{R}_0 quantifies a disease’s potential to be transmitted within a population and it is used to describe the contagiousness of the infectious disease. This concept was developed by Van den Driessche and Walmough (2002) and is calculated as the largest eigenvalue of the next- generation matrix.

Theorem 2.3. The model (2) has the following basic reproduction number \mathfrak{R}_0 :

$$\mathfrak{R}_0 = \frac{\beta\mu(\sigma + \nu + \mu)}{(q + \mu)(\sigma + \nu + \mu) - \sigma q} \cdot \frac{\alpha}{(\alpha + \mu)(\gamma + \mu + \delta)} \tag{9}$$

Proof 2.3. Each element of the next generation matrix represents the rate of transmission between compartments. The next generation matrix can be derived from two matrices denoted as \mathfrak{Z} and Υ . The matrix $\mathfrak{Z}(x)$ gives the rate of new infection appearances and the matrix $\mathfrak{Z}(x)$ gives the rate of individuals’ transition in and out of compartments.

Because $X = (S, E, I, R, V, D)^T$ for model (2) follows:

$$\frac{dX}{dt} = \mathfrak{Z}(x) - \Upsilon(x)$$

Where: $\mathfrak{Z}(X) = \begin{bmatrix} 0 \\ \frac{\beta SI}{N} \\ 0 \\ 0 \\ 0 \\ 0 \end{bmatrix}$, and $\Upsilon(X) = \begin{bmatrix} \frac{\beta SI}{N} + qS + \mu S - \sigma V - \Lambda \\ (\alpha + \mu)E \\ (\gamma + \delta + \mu)I - \alpha E \\ \mu R - \gamma I - \nu V \\ -(\sigma + \nu + \mu)V - qS \\ -\delta I \end{bmatrix}$

The Jacobian matrix is obtained from two matrices F and V . The elements in new infection matrix F represent the flow of new infections in the model and the elements of transition or recovery matrix V gives the flow of individual leaving the compartments. If the equilibrium point is applied in model (2) these matrices are:

$$F(X^*) = \begin{bmatrix} 0 & \frac{\beta S}{N} \\ 0 & 0 \end{bmatrix}$$

and

$$V(X^*) = \begin{bmatrix} \alpha + \mu & 0 \\ -\alpha & \gamma + \delta + \mu \end{bmatrix}$$

In Theorem 2.1. for the total population was proven that $N \leq \frac{\Lambda}{\mu}$. In the equilibrium point,

the total population is $N = \frac{\Lambda}{\mu}$, so that $F(X^*) = \begin{bmatrix} 0 & \frac{\beta \mu S}{\Lambda} \\ 0 & 0 \end{bmatrix}$.

For the next generation matrix is obtained:

$$FV^{-1} = \begin{pmatrix} 0 & \frac{\beta \mu (\sigma + \nu + \mu)}{(q + \mu)(\sigma + \nu + \mu) - \sigma q} \\ 0 & 0 \end{pmatrix} \begin{pmatrix} \frac{1}{\alpha + \mu} & 0 \\ \frac{\alpha}{(\alpha + \mu)(\gamma + \mu + \delta)} & -\frac{1}{\gamma + \mu + \delta} \end{pmatrix}$$

Thus, the theorem 2.3 is proved.

Theorem 2.4. If $\mathfrak{R}_0 > 1$, the disease-free equilibrium point (7) is unstable, indicating that the disease is transmitting within given population. Conversely, if $\mathfrak{R}_0 < 1$, the disease-free equilibrium point (7) is asymptotically stable, suggesting that the disease will eventually die out in the population.

Proof 2.5. The Jacobian matrix of model (2) is:

$$J = \begin{pmatrix} -\frac{\beta I}{N} - (q + \mu) & 0 & -\frac{\beta S}{N} & 0 & \sigma & 0 \\ \frac{\beta I}{N} & -(\alpha + \mu) & \frac{\beta S}{N} & 0 & 0 & 0 \\ 0 & \alpha & -(\gamma + \delta + \mu) & 0 & 0 & 0 \\ 0 & 0 & \gamma & -\mu & \nu & 0 \\ q & 0 & 0 & 0 & -(\sigma + \nu + \mu) & 0 \\ 0 & 0 & \delta & 0 & 0 & 0 \end{pmatrix}$$

The Jacobian matrix at DFEP is:

$$J(X^*) = \begin{pmatrix} -(q + \mu) & 0 & -\frac{\beta\mu S^*}{\Lambda} & 0 & \sigma & 0 \\ 0 & -(\alpha + \mu) & \frac{\beta\mu S^*}{\Lambda} & 0 & 0 & 0 \\ 0 & \alpha & -(\gamma + \delta + \mu) & 0 & 0 & 0 \\ 0 & 0 & \gamma & -\mu & \nu & 0 \\ q & 0 & 0 & 0 & -(\sigma + \nu + \mu) & 0 \\ 0 & 0 & \delta & 0 & 0 & 0 \end{pmatrix}$$

It is essential to ensure all the eigenvalues of Jacobian $J(X^*)$ are negative. For this purpose, the characteristic equation $\det(J(X^*) - \lambda E) = 0$ is considered. Calculating this determinant, follows that:

$$\lambda(\lambda + \mu)(\lambda^2 + (A + F)\lambda + AF - \sigma q)(\lambda^2 + (B + C)\lambda + BC - \alpha G) = 0$$

Where $A = q + \mu$, $B = \alpha + \mu$, $C = \gamma + \delta + \mu$, $F = \sigma + \nu + \mu$ and $G = \frac{\alpha\beta\mu S^*}{\Lambda}$.

Because $\alpha, \beta, \gamma, \delta, q, \nu, \sigma, \Lambda, \mu, S^* > 0$, it follows that $A, B, C, F, G > 0$. For simplification, \mathfrak{R}_0 and S^* expressed by A, B, C, F, G are given with the following equations:

$$\mathfrak{R}_0 = \frac{\beta\mu(\sigma + \nu + \mu)}{(q + \mu)(\sigma + \nu + \mu) - \sigma q} \cdot \frac{\alpha}{(\alpha + \mu)(\gamma + \mu + \delta)} = \frac{\beta\mu F}{AF - \sigma q} \cdot \frac{\alpha}{BC}$$

and

$$S^* = \frac{\Lambda(\sigma + \nu + \mu)}{(q + \mu)(\sigma + \nu + \mu) - \sigma q} = \frac{\Lambda F}{AF - \sigma q}$$

The following eigenvalues of $J(X^*)$ are obtained:

$$\begin{aligned}\lambda_1 &= 0 \\ \lambda_2 &= -\mu < 0 \\ \lambda_3 &= \frac{-(A+F) - \sqrt{(A+F)^2 - 4(AF - q\sigma)}}{2} \\ \lambda_4 &= \frac{-(A+F) + \sqrt{(A+F)^2 - 4(AF - q\sigma)}}{2} \\ \lambda_5 &= \frac{-(B+C) - \sqrt{(B+C)^2 - 4(BC - \alpha G)}}{2} \\ \lambda_6 &= \frac{-(B+C) + \sqrt{(B+C)^2 - 4(BC - \alpha G)}}{2}\end{aligned}$$

Now, the eigenvalues λ_5 and αG are estimated. In the quadratic equation $\lambda^2 + (A+F)\lambda - \sigma q = 0$ for the coefficients are true $A+F > 0$ and $AF - q\sigma > 0$. It is clear that $A+F > 0$, while for $AF - q\sigma > 0$ is obtained:

$$AF - q\sigma = (q + \mu)(\sigma + \nu + \mu) - q\sigma = q\sigma + q\nu + q\mu + \mu\sigma + \mu\nu + \mu^2 - q\sigma > 0$$

Lemma 2.1. The discriminant of the quadratic equation

$$\lambda^2 + (B+C)\lambda + BC - \alpha G = 0$$

is greater than zero, for every value of $\alpha, \beta, \gamma, \delta, q, \nu, \sigma, \Lambda, \mu$.

Proof Lemma 2.1. It is clear that:

$$\det = (B+C)^2 - 4(BC - \alpha G) = (B-C)^2 + 4\alpha G > 0$$

and $\lambda_5, \lambda_6 \in \mathbb{R}$ thus $\lambda_5 < 0$. The sign of λ_6 depends on:

$$\sqrt{(B+C)^2 - 4(BC - \alpha G)} \leq B+C$$

Or

$$\sqrt{(B+C)^2 - 4(BC - \alpha G)} > B+C$$

The equation $\lambda^2 + (B+C)\lambda + BC - \alpha G = 0$ can be transformed as:

$$\lambda^2 + (B+C)\lambda + \frac{\alpha G(1 - \mathfrak{R}_0)}{\mathfrak{R}_0} = 0$$

The last equation is correct because of $\frac{\alpha G(1 - \mathfrak{R}_0)}{\mathfrak{R}_0} = \frac{\alpha G}{\mathfrak{R}_0} - \alpha G$ and

$$\frac{\alpha G}{\alpha G} = \frac{\frac{\alpha\beta\mu S^*}{\Lambda}}{\frac{\alpha\beta\mu F}{(AF - \sigma q)BC}} = \frac{\frac{\alpha\beta\mu F}{AF - \sigma q}}{\frac{\alpha\beta\mu F}{(AF - \sigma q)BC}} = BC$$

If $\mathfrak{R}_0 < 1$ than $\sqrt{(B+C)^2 - 4(BC - \alpha G)} \leq B+C$, because the eigenvalue $\lambda_6 < 0$ and the equilibrium point X^* is considered to be locally asymptotically stable. If $\mathfrak{R}_0 > 1$ than $\sqrt{(B+C)^2 - 4(BC - \alpha G)} > B+C$ because the eigenvalue $\lambda_6 > 0$, then the equilibrium point X^* is locally asymptotically unstable.

3. Results and discussion

The analysis is conducted with data obtained from Public Health Institute of North Macedonia (2023). The model was simulated using AnyLogic® software and the effects of different values of some parameters with graphical interpretations have been analyzed. Each compartment: susceptible (S), exposed (E), Infected (I), Recovered (R), Vaccinated (V) and Death (D) can be represented by state chart in AnyLogic®. The chart defines the transmission between states over time. The parameters used in the simulation are dynamic and during the simulation their impact can be evaluated. AnyLogic uses time-series plots for data visualization for all compartments. Additionally, with AnyLogic® multiple scenarios can be tested, such as different vaccination rate, transmission rate etc. These parameters can be adjusted to assess how their change affects the outcome of the pandemic. The total population in North Macedonia is 2114176 (Macrotrends, 2024). The natural mortality rate per capita is 0.013 and the recruitment of susceptible population is 21960 (Macrotrends, 2023). The period of incubation for measles is from 10 to 14 days but can extend up to 21 days. The recovery period is from 2 to 3 weeks, so the recovery rate has been set

as $\frac{1}{\tau_{recovery}} = \frac{1}{14} = 0.071$. According to Public Health Institute (2023) in 2018 North Macedonia

had a measles-related mortality rate of 2 deaths per 1000 infected individuals. That year, the vaccination rate in North Macedonia is 74.4% with 99.2% of those vaccinated developing immunity. In Table 1 are listed all the parameters with their values.

Parameter	description	value
Λ	Susceptible recruitment	21960
β	Transmission rate	0.6-0.9
α	Exposure rate	0.100
γ	Recovery rate	0.071
δ	Mortality rate of measles	0.002
q	Vaccination rate	0.744-0.96
ν	Immunity development rate	0.992
σ	Ineffective vaccination rate	0.008
μ	Natural mortality rate	0.013

Table 1. Description and estimated values of parameters.

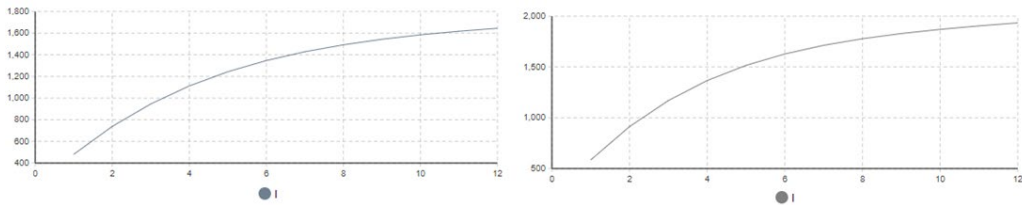


Fig. 2. Number of infected individuals for transmission rate a) $\beta = 0.6$ and b) $\beta = 0.9$ for vaccination rate $q = 0.744$

In Figure 2, the variations are represented of the number of infected persons for the developed model (2) for the period of 12 months when the vaccination rate is 0.744 or 74.4% and variable transmission rates. When the transmission rate is set to be 0.6, the number of annual infected individuals is little above 1600 individuals, as shown in Figure 2(a), whereas when the transmission rate is increased to 0.9, the annual number of infected individuals increases to a value under 2000 infected individuals. Figure 2 shows that at the end of the year, the number of infected persons is higher if the transmission rate is increased.

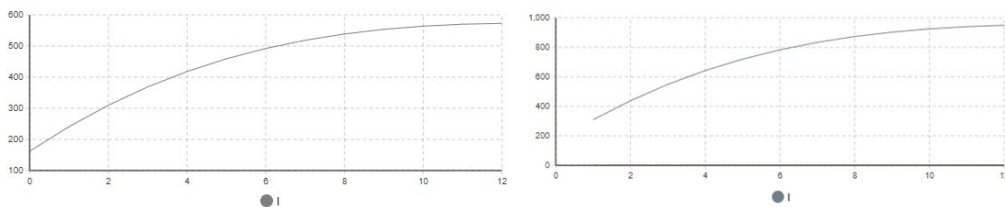


Fig. 3. Number of infected individuals for transmission rate a) 0.6 and b) 0.9 for vaccination rate $q = 0.950$

WHO (2019) recommends a vaccination rate over 0.95 for herd immunity and elimination of measles. Therefore, the next set of simulation was conducted with vaccination rate 0.95. All

other values of the model (2) are set as in Table 1. When the transmission rate is 0.9, the annual number of infected individuals remains below 1000. However, when the transmission rate decreases to 0.6, the number of infected individuals per year decreases to under 600 individuals. Figure 2 and Figure 3 demonstrate that reducing the transmission rate decreases measles transmission. In high-density areas, close contact between individuals increases transmission risk, necessitating social distancing and public health measures. Higher vaccination rate reduces the number of susceptible individuals, lowering transmission and overall measles spread. Also, the highly effective measles vaccine significantly reduces the number of infected individuals. Figure 4 compares the number of measles-related deaths for a constant transmission rate $\beta = 0.6$, showing a decrease in deaths with higher vaccination rate.

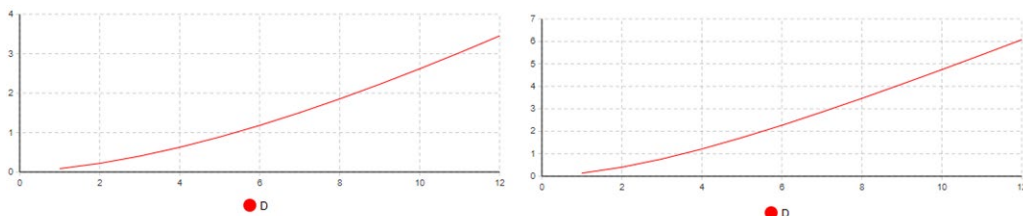


Fig. 4. Number of deceased individuals for transmission rate $\beta = 0.6$ and vaccination rates a) 0.950 and b) 0.744

4. Conclusions

In this paper, SEIRV+D model was developed to investigate measles' dynamics within a given population. First, the equilibrium point was derived, and then the expression for the reproduction number is presented. The stability of the equilibrium is assessed based on reproduction number.

The advantages of this model are based on the fact that it combines many important components that make it adaptable to real-world scenarios compared to traditional SEIR models. The proposed model improves upon simple models like SIR and SEIR by introducing more compartments and considering additional rates. Compared to static models, this model also considers birth rates and mortality rates, maintaining the model's dynamic nature. Unlike the dynamic SEIRV model, this model considers natural mortality, which is not caused by measles, making it adaptable to dynamic populations. It also considers the success of vaccination, making the model more realistic and predicting the impact of vaccination.

This model includes a vaccination compartment, where individuals transition from susceptible to vaccinated, and if the vaccination is successful, they move to the recovered state. Otherwise, they return to the susceptible state, allowing for dynamic adjustments of vaccination rates. This can influence vaccination campaigns by demonstrating the significance of vaccination and its impact on disease transmission and immunity. It can be emphasized that these elements facilitate better forecasting, planning, and policymaking in public health.

The case study is based on real data from Public Health Institute of North Macedonia. The simulations were conducted with varying transmission and vaccination rates. The transmission rate, a critical parameter, quantifies how quickly measles spreads from infectious to susceptible individuals. It is directly linked to the contact rate and represents the frequency of interactions leading to measles transmission. Results show that at a vaccination rate of 0.744 and transmission rate 0.6 the annual number of infected individuals is slightly above 1600. Increasing the vaccination rate to 0.95 for the same transmission rate, the annual number of infections is reduced

to under 600. For a higher transmission rate ($\beta=0.9$), infection decreases from nearly 2000 at vaccination rate 0.744 to below 1000 for vaccination rate 0.95. At vaccination rate 0.744, measles-related deaths remain higher for all transmission rates, reflecting the vulnerability of a larger susceptible population. When vaccination rate reaches 0.95, annual deaths for transmission rate of 0.9 are significantly reduced, aligning with the WHO's goal for measles elimination.

The deployed SEIRV+D model proves highly effective in quantifying the combined impact of vaccination, transmission reduction, and annual mortality. It highlights that achieving vaccination coverage above 95% and maintaining low transmission rate is critical to minimizing the number of infected individuals and measles-related deaths.

In summary, the model indicates that North Macedonia can achieve significant progress toward measles elimination by improving vaccination coverage, implementing public health measures, and maintaining effective immunization programs.

References:

- Al- Darabsah I (2021). A time- delayed SVEIR model for imperfect vaccine with a generalized nonmonotone incidence and application to measles, *Applied Mathematical Modelling*, 91, 74-92.
- Arsal S R, Alida D, Handari B D (2020). Short review of mathematical model of measles. *AIP Conference* 2264, 020003.
- Bailey A, Sarpa A (2023). *MMR Vaccine*, StatPearls Publishing, Treasure Island.
- Berche P (2022). History of measles, *La Presse Médicale*, 51.
- Centres for Disease Control and Prevention (2021). *Epidemiology and prevention of vaccine-preventable diseases*. 14th Edition, Public Health Foundation, Washington DC.
- Driessche P, Waltmough J (2002). Reproduction numbers and sub- threshold endemic equilibria for compartment models of disease transmission, *Mathematical Bioscience*, 180, 29-48.
- Griffin D E (2016). The immune response in measles: virus control, clearance and protective immunity, *Viruses*, 8, No. 10.
- Hajii M E, Albarg A H (2022). A mathematical investigation of SVEIR epidemic model for the measles transmission. *Mathematical Biosciences and Engineering*, 19(3).
- Kermack W O, McKendrick A G (1991). Contributions to the mathematical theory of epidemics, *Bull. Math. Biol.*, 53, No. 12.
- Kukusheva Paneva M, Stojkovikj N, Martinovska Bande C, Koceva Lazarova L. (2024). Mathematical analysis and simulation of measles infection spread with SEIRV+D model. *ICT Innovation 2023*, web proceedings. pp.39-47
- Kukusheva Paneva M, Stojkovikj N, Zlatanovska B, Koceva Lazarova L, Stojanova Ilievska A, Martinovska Bande C (2024). Modelling and simulation of susceptible- exposed- infected- recovered- vaccinated- susceptible model of Influenza. *TEM Journal*, 13, 663- 669.
- Lau M, Becker A, Madden W, Metcalf C, Grenfell B T (2022). Comparing and liking machine learning and semi-mechanical models for predictability of endemic measles dynamics. *PLoS Comput Biol*, 18, No. 9.
- Microtrends (2024), <https://www.macrotrends.net/global-metrics/countries/mkd/macedonia/life-expectancy> last access 2024/07/10.
- Monoh A, Ibrahim M, Uwanta I, Manga S (2013). Mathematical model for control of measles epidemiology, *International Journal of Pure and Applied Mathematics*, 87, 707-717.
- Moss W J, Griffin D E (2006). Global measles elimination. *Nat Rev Microbiol*, 4, No 12:900-8.
- Ottar N, Rnstad B J O, Inkenstadt B F, Grenfell B (2002). Dynamics of measles epidemics: estimating scaling of transmission rates using a time series SIR model. *Ecological Monographs*, 72, No. 2, 169-184.

-
- Public Health Institute of Republic of North Macedonia (2023). Trends in acute infectious diseases in North Macedonia in 2022.
- Stojkovikj N, Kukusheva Paneva M, Zlatanovska B, Koceva Lazarova L (2024). Modelling, analysis and simulation of tuberculosis. *Asian- European Journal of Mathematics*, 17, No. 9.
- World Health Organization (2019). Measles vaccines: WHO position paper- recommendations, vaccine, 32, No.2.
- World Health Organization (2019). Measles vaccines: WHO position paper- recommendation, vaccine, 37, No. 2, 219-222.
- Worldometer (2023). North Macedonia Population (2021)- Worldometer (worldometers.info) last access 2023/09/29.
- Zaman G, Kang H, Cho G, et al. (2017). Strategy of vaccination and treatment in an SIR epidemiology model, *Mathematics and Computer in Simulation*, 136, 63-77.